Study of the mechanical properties of Ti_2AlC after thermal shock

V. Adamaki[1], T. Minster[2], G. Fourlaris[2], C. R. Bowen[1]
[1] Mechanical Engineering department, University of Bath, UK
[2] College of Engineering, Swansea University, UK

Abstract

The ternary carbides and nitrides, known as MAX phases combine the attractive properties of both ceramics and metals; for example the Ti_2AlC ceramics examined in this work have attracted attention for high temperature applications such as aerospace engines. In the current work Ti_2AlC ceramics were subjected to high levels thermal shock from temperatures of 1200^{o}C with a cooling rate of more than 90^{o}C/sec. After the thermal shock process the mechanical properties and the microstructure were investigated. Combined thermal shock and mechanical loading with an applied stress of 0, 50, 100 and 150 MPa was examined and in all cases the samples maintained their microstructure without any micro-cracks or phase change observed. Compression testing of all samples to failure indicated that their mechanical properties did not show any deterioration in the testing range examined. Such ceramics materials therefore show potential for high temperature and high load applications.

Keywords: MAX phases, mechanical properties, thermal shock

Introduction

Ti_2AlC is one of the particular MAX phases ceramics that have attracted significant interest due to their unique behaviour that provides it with properties and attributes that are characteristic of both metals and ceramics. Ti_2AlC is a ternary carbide that belongs to a larger class of ceramics with a general formula $M_{n+1}AX_n$, where *n*=1-3, *M* is an early transition metal, *A* is an A-group element and *X* is carbon or nitrogen. These ceramics are intriguing as they are electrically and thermally conductive [1], damage tolerant and readily machinable while also exhibiting high temperature resistance. The Ti_2AlC is of particular interest since it has excellent oxidation resistance due to it being an alumina former which provides it with some protection to oxidation [2]; this allows it to be used in high temperature applications while maintaining its mechanical properties. In addition, the density of Ti_2AlC is relatively low [2], 4.11 g/cm^3, which is beneficial when it is used as a structural material for aerospace application requiring low mass.

A variety of methods have been reported to manufacture high purity and high density Ti_2AlC samples with the most successful being hot isostatic pressing (HIP) [3-7]. The disadvantage of the HIP process is that it can be time consuming and requires a relatively high level of energy input. Additional work has examined pressureless sintering (PS) that can be more suitable for mass production of mechanical parts with complex shapes [7], but the materials are typically more porous/lower density.

Since the Ti_2AlC materials are good conductors of heat (46 W/mK [8]) and electricity ($3x10^6$ $\Omega^{-1}m^{-1}$ [1]), they are promising candidates as heating elements and electrodes [9, 10]. Their ability to provide high temperature mechanical properties makes it clear that that MAX phase ceramics have the potential for high temperature applications such as aerospace engines where the efficiency is strongly related to operating temperature [2].

Previous studies on the mechanical properties of Ti_2AlC have included room temperature assessment of the mechanical properties. Wang *et al.* measured compressive strength of 670MPa and a Vicker's hardness was 4.2-5.7 MPa [11]. These promising mechanical properties are a result of the localised lattice distortions that allow the delamination of multiple layers of the structure. Zhou *et al.* [12] studied the mechanical properties of Ti_2AlC through compression testing from room temperature up to 1200^oC, reporting a change in the plasticity and strength above 1000^oC where the stress upon failure decreased indicating that the material deformed with some degree of plastically. Bai *et al.* measured a flexural strength of 432 MPa by conducting three-point bending test from room temperature up to 950^oC and observed a change in plasticity above 750^oC [8].

While a limited amount of work has undertaken mechanical testing, less has examined thermal shock behaviour. This work therefore focuses on studying the mechanical properties of Ti_2AlC after thermal shock under mechanical stress. The samples are heated up to temperatures of 1200^oC and the then quenched to evaluate their resistance in thermal shock. To the best of our knowledge this is the first work on studying the mechanical properties of Ti_2AlC after thermal shock and is of particular importance for applications such as furnace elements or aerospace components at high temperature where there is significant potential for such loading conditions to occur.

Experimental methods

The material used in this work is commercial polycrystalline Ti_2AlC from Kanthal (Kanthal, Sweden) with density of 4.2 g/cm^3 [13], prepared via HIP. The samples for the mechanical testing were cylinders of 10 mm in diameter and 15 mm in height. Due to the high electrical conductivity of the Ti_2AlC ceramic the thermal shock was performed on a Gleeble 3500 dynamic system (Dynamic Systems Inc.). The systems uses direct resistance heating with high thermal conductivity grips to hold the specimen for high heating and cooling rates [14]; such an approach to high temperature testing in not feasible on conventional electrically insulating ceramics. Fig. 1 presents a schematic representation of the Gleeble testing set up to test the ceramics.

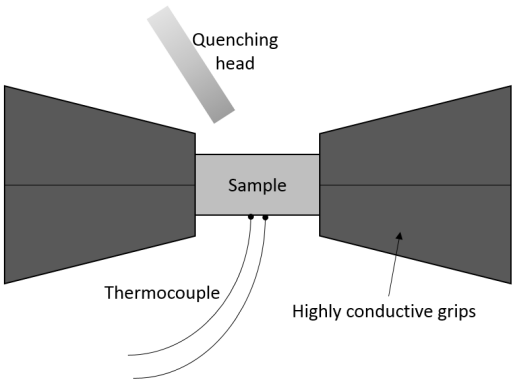

Figure 1: Schematic representation of the Gleeble testing set up. Electrically conductive grips allow Joule heating of the ceramic materials.

The thermal shock cycle involved heating the sample to a temperature of 1200^{o}C and the cooling of the materials at cooling rates above 90 ^{o}C/sec using quenching with gas. The temperature of 1200^{o}C was chosen since its well above the sintering temperature, but above the brittle-to-ductile transition detected in previous work [8, 12]. Thermocouples were attached to the Ti_2AlC to provide feedback control of specimen temperatures during resistive heating. While quenching the material to induce a thermal shock a compressive load of 0, 50, 100 or 150 MPa was applied on the materials. In order to investigate any potential changes in the mechanical properties the strain was also recorded while heating up and cooling. After thermal shock the samples were as subjected to compression testing (Instron 5585H) to study the residual mechanical properties. A control sample that was not subjected to any mechanical load or thermal shock treatment was also tested. Complementary, dilatometry measurements using a DIL 402C Netzsch were performed allowing the measurement of the expansion of the material from room temperature up to 1200^{o}C to detect potential phase changes in the materials or changes in the thermal expansion with temperature. Density measurements were conducted based on the BS EN623:2 standard [16] to determine the density of the samples before testing. Scanning electron microscopy (SEM) was also undertaken to examine the microstructure using a JEOL JSM6480LV and Field emission SEM (FESEM) was used to examine the nanostructure (JEOL JSM-6301F). Energy dispersive X-ray (EDX) was also undertaken in an SEM JEOL 6480 for an elemental analysis of the specimen. Finally, X-ray diffraction (XRD) was conducted to detect any phase changes in the samples due to the high temperature heat treatment, using a Phillips PW1730 (Cu-Kα, λ=1,541838Å, 40kV, 25mA).

Results and discussion

XRD and microstructure

X-ray diffraction prior to thermal shock confirmed the presence of the dominant phase of Ti_2AlC, as shown in Fig. 2a, along with the presence of the secondary phases

consisting of $AlTi_3$ and TiC; such secondary phases are commonly observed in these materials [7, 16-17]. The bulk density measured by the Archimedes method was 96.6% of the theoretical (0.23% apparent solid porosity) which agrees with the high density microstructure in Fig. 2b. The FESEM image in Fig. 2b shows the sample microstructure prior to thermal shock and shows characteristic [18-19] large size grains, with average length of 30.9 μm and thickness of 6.2 μm that are composed of a number of micro-laminates (Fig.1b inset). There are no microcracks visible before the thermal shock as observed.

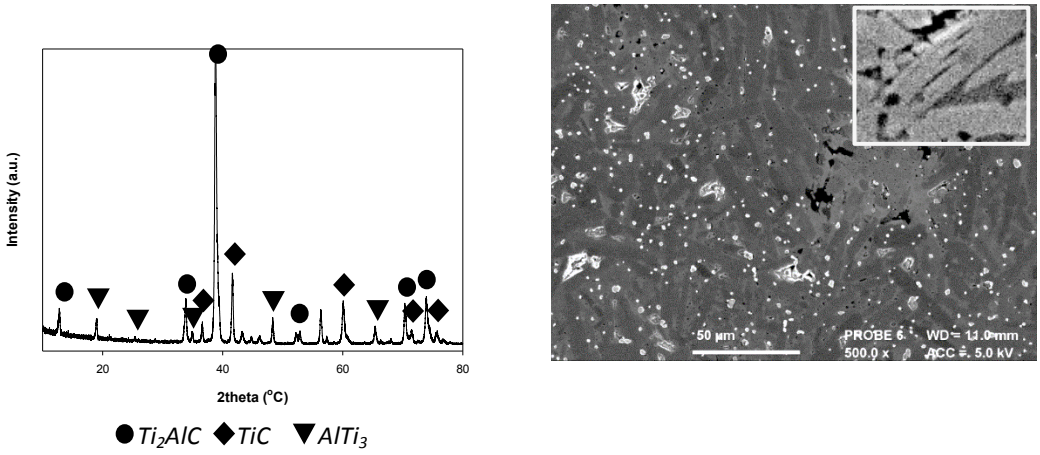

a *b*

Figure 2: a. XRD spectrum, b. FESEM image of Ti_2AlC before the thermal shock

EDS was conducted to determine the location of the Ti_2AlC, TiC and $AlTi_3$ phases and Fig. 3a shows the mircostructure and Fig 3b shows the EDS spectra from a variety of sites of interest indicated in Fig. 3a. The dominant phase of Ti_2AlC is present in the characteristic long grains, whereas TiC seems to form a second phase that appears darker in the SEM image, since Spectrum 5 shows a lower content of Al. The $AlTi_3$ is present in the grain boundaries (see Spectrum 2 & 3).

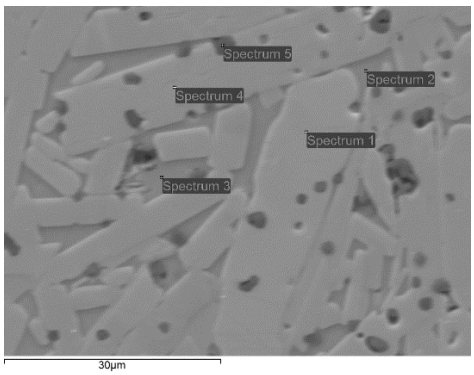

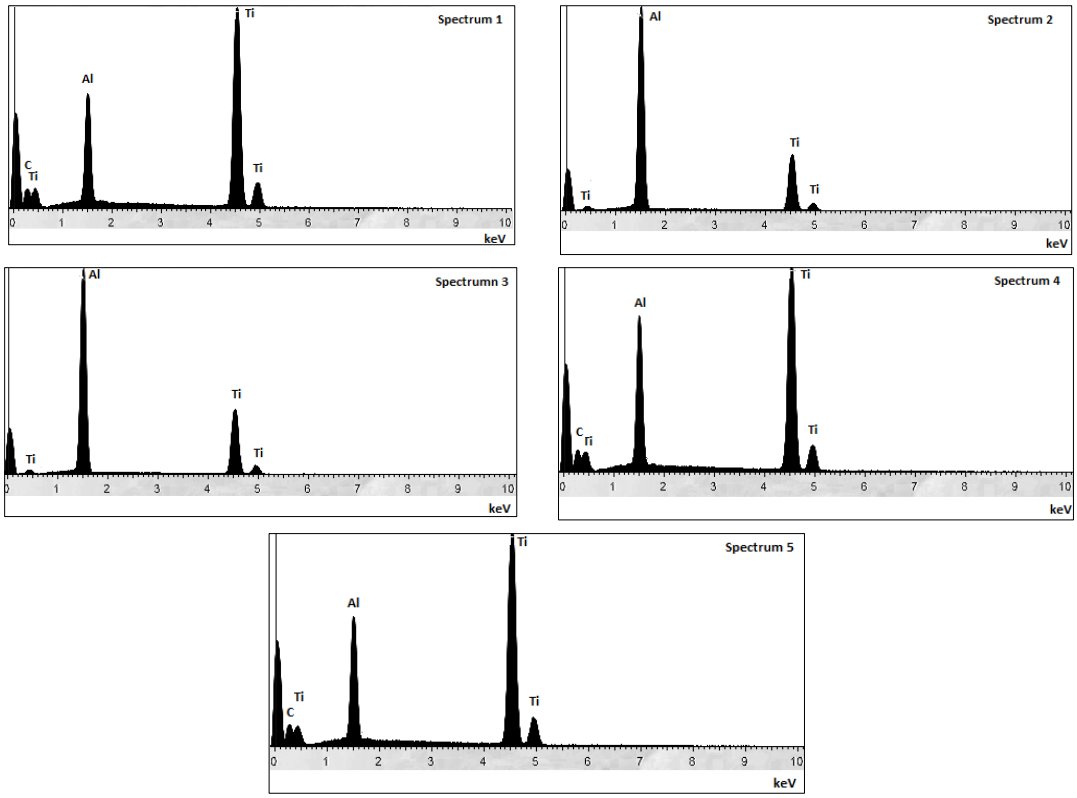

Figure 3: Site of interest and EDS spectrums of the MAX phase samples before the thermal shock

Room temperature compression testing

Compression testing before thermal shock was performed in order to determine the applied stress (strength), this was 722.3 MPa (Fig. 4a). This value agrees with reported values of the mechanical properties [11-12]. The failure mechanism of the material is shown in Fig. 4b is not characteristic of a typical brittle ceramic material and that indicates ductile nature of Ti_2AlC. This cross-shape formation is characteristic of quasi-brittle or composite materials [20]. The yield and fracture occur in a band, oriented at about 45^o with respect to the loading axis. One face is stiffer, whereas the other phase of lower strength endows the material with ductility [21]. Fig. 5 shows a schematic of the failure mode of quasi-brittle (Fig. 5a) and brittle (Fig. 5b) materials.

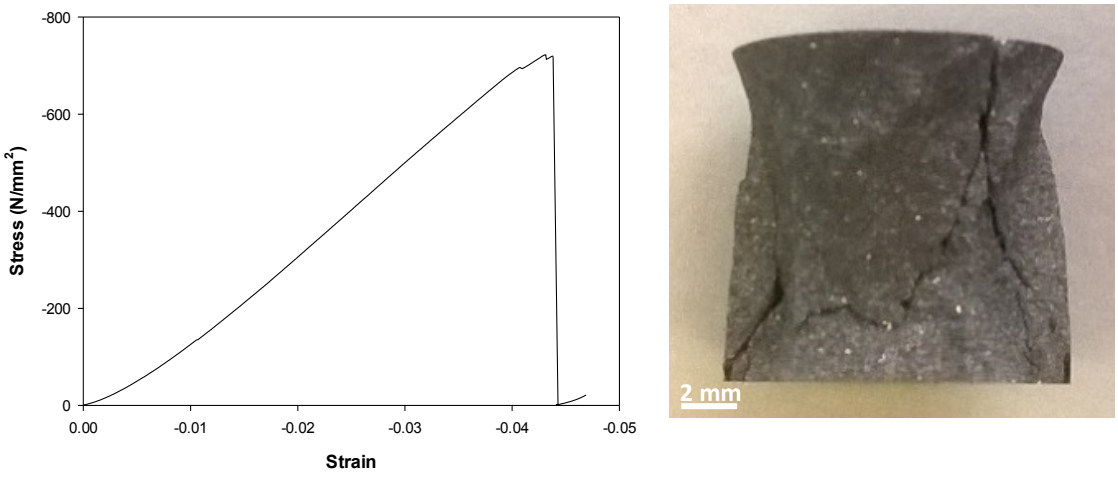

a *b*

Figure 4: a. Compression test stress-strain curve of Ti_2AlC before the thermal shock, b. Image of sample after failure, sample diameter is 10mm for scale

a *b*

Fig. 5: Failure mode of (a) quasi brittle and (b) brittle samples under compressive test

Thermal shock testing

Fig. 6 shows the thermal profile during thermal shock testing. Initially, the samples were heat to temperatures of up to 1200^{o}C at a rate of 10 ^{o}C/sec and maintained at elevated temperature for 20s to attain equilibrium. Then, the samples were rapidly cooled by quenching with cooling rate between 60-90^{o}C/sec from 1200^{o}C down to 850^{o}C. The cooling rate decreases as it approaches room temperature. The first sample was heated to a temperature of 1200^{o}C and then during quenching no load was applied. Fig. 7a and 7b shows the strain recorded during heating up and during quenching. In Fig. 7a there is a change in the strain slope around 700^{o}C that may indicate a phase change or a change in the deformation mechanism. A change in the strain slope is also observed during quenching as shown in Fig. 7b at around 1100^{o}C. Fig. 8 shows the XRD data and an SEM image after the thermal shock with no load applied. Ti_2AlC is shown as the dominant phase present in the XRD spectrum and no microcracks are visible in the microstructure after the thermal shock. According to Zhou et al. [12] the Ti_2AlC undergoes a brittle-to-ductile-transition (BDTT) at 1050^{o}C

at which the deformation mechanism changes and the availability and the mobility of grain boundaries contribute to a more ductile behaviour. Therefore the strain change at approximately 1050°C that was observed during quenching may be attributed to the BDTT. However, Y. Bai *et al.* studyied the mechanical properties of the materials and detected a BDTT at approximately 750°C [8]. Recently R. Benitez *et al.* published work on Ti_2AlC hysteresis loops in the stress-strain curve as a result of elastic-plastic anisotropy due to the different orientation of the grains [22]. A possible explanation of this difference of the BDTT temperature during heating and cooling could be a change of the orientation of the grains in high temperature.

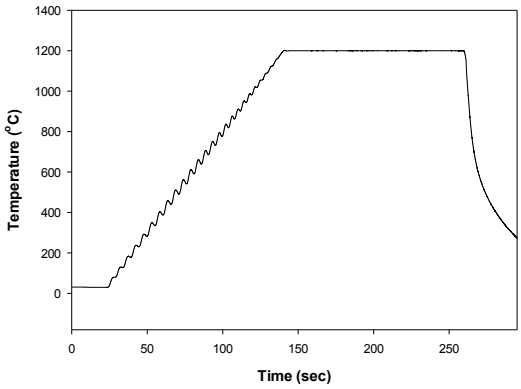

Figure 6: Temperature profile while heating up and cooling down by quenching

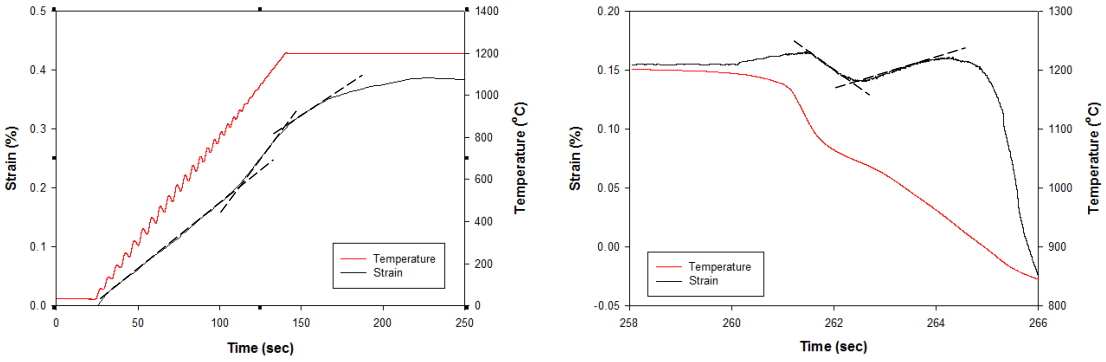

a *b*

Figure 7: a. Heating ramp before the thermal shock, b. Temperature vs time (right axes) and strain vs time (left axes) during quenching

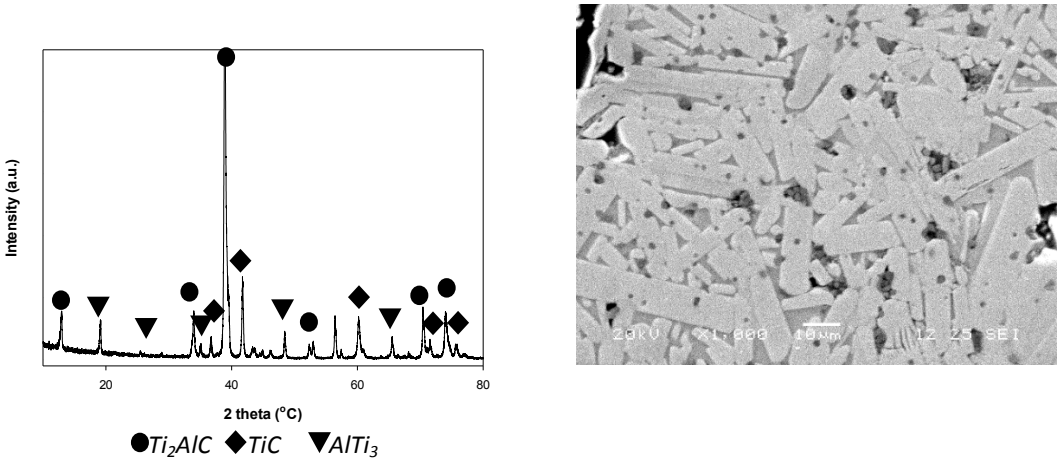

Figure 8: a. XRD spectrum and b. SEM image of the Ti_2AlC after the thermal shock without any load applied

No phase change is detected, but the dilatometry data can confirm the change in the deformation mechanism. Fig. 9 shows the dilatometry data and presents temperature, expansion (dl/l_0) and the 1st derivative of the expansion vs time. Although there is no significant change in the dl/l_0 (%), a closer look at the first derivative shows a change in the slope of the dl/l_0 (%) at approximately 950°C during heating and at approximately 850°C when cooling. These temperatures are slightly different to those reported from Zhou *et al* [12] and Bai *et al* [8] and the temperatures spotted during quenching. Different grain orientation could be the cause of the differences in the temperature that the deformation mechanism changes.

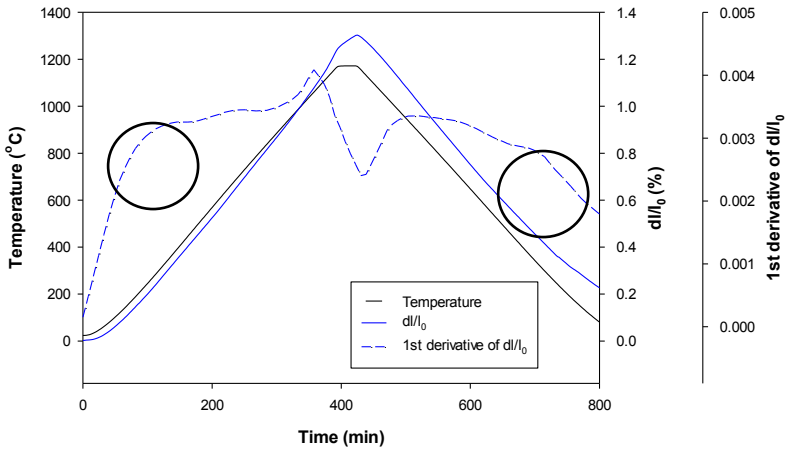

Figure 9: Temperature, expansion and 1st derivative of the expansion vs time, data obtained from dilatometry

The heating and quenching cycles using the Gleeble were applied to three more samples under load, with an applied compressive stress of 50, 100 and 150 MPa applied respectively on the samples. Figure 10a, b and c show the strain vs time

graph during the thermal shock from 1200°C. In this case the strain decreases with reduction in temperature, possibly because of the additional load applied.

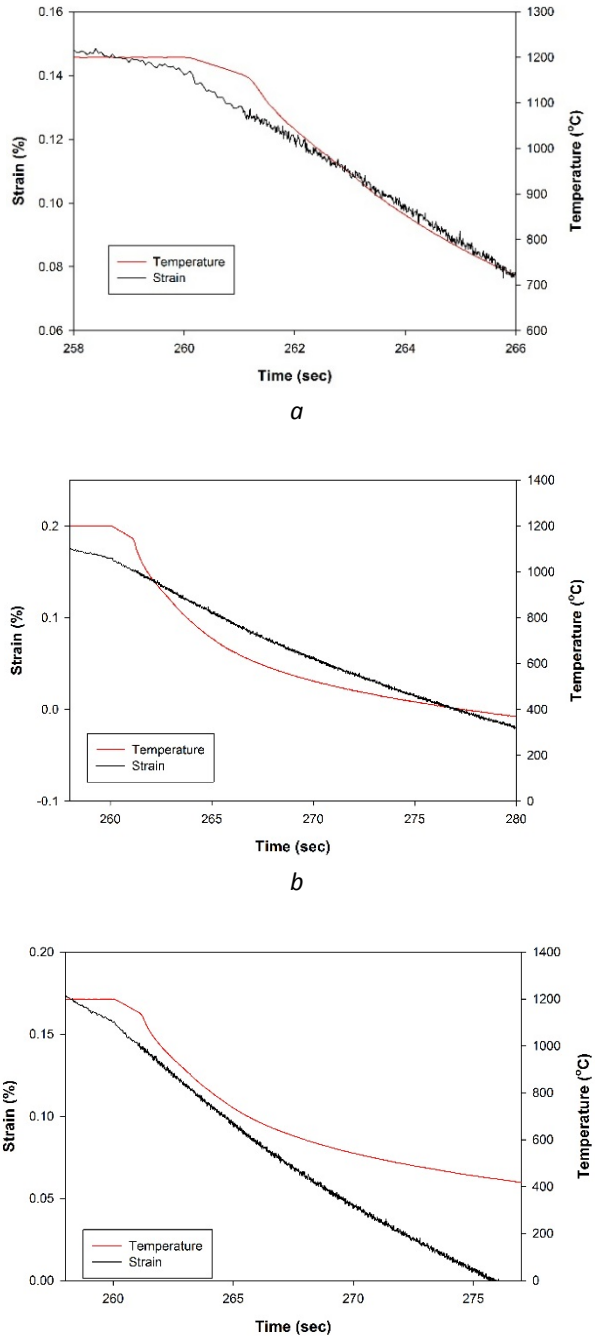

Figure 10: Temperature vs time (right axes) and strain vs time (left axes) during quenching of the samples that a load of a. 50 MPa, b. 100 MPa and c. 150 MPa was applied

As shown from the XRD spectra in Fig. 11 there are changes in the phase composition due to the thermal treatment or load applied during quenching. A semi-quantitive analysis was performed by calculating and comparing the integrated area of the main peaks of the three phases present (38° for the Ti_2AlC, 41° for TiC and 48°

for $AlTi_3$). The SEM images in Fig. 12 shows that again there are no cracks observed in the microstructure as result of the combination of applied mechanical load and thermal shock.

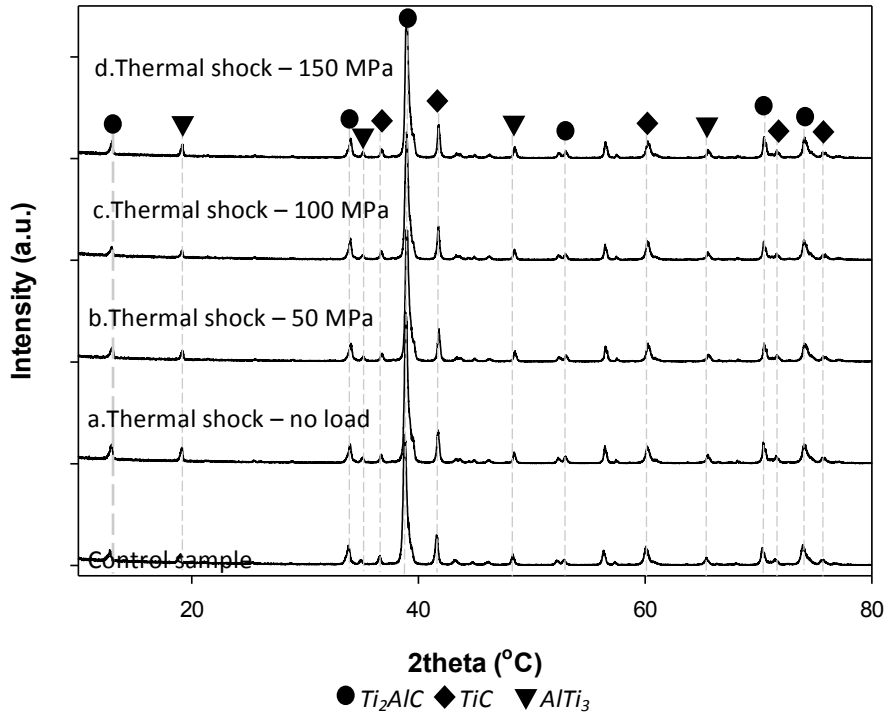

Figure 11: XRD spectra after the thermal shock of the samples that a load of a. 0 MPa, b. 50 MPa and c. 100 MPa and d. 150 MPa was applied during quenching

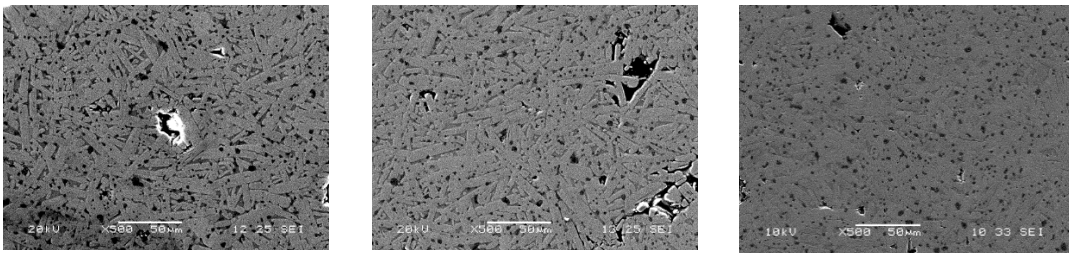

a *b* *c*

Figure 12: SEM after the thermal shock of the samples that a load of a. 50 MPa, b. 100 MPa and c. 150 MPa was applied during quenching

Residual strength testing after thermal shock

Following the thermal shock and combined thermal shock and mechanical loading the materials were subjected to compression testing to investigate any possible effects of reduction in strength. Fig. 13 shows the compression test of the control sample (no thermal shock) and all the samples after being subjected to thermal shock under 0, 50, 100 and 150MPa. Table 1 also compares the results showing that

no significant changes in the maximum strength are observed, any difference in the values is within the uncertainties of the test.

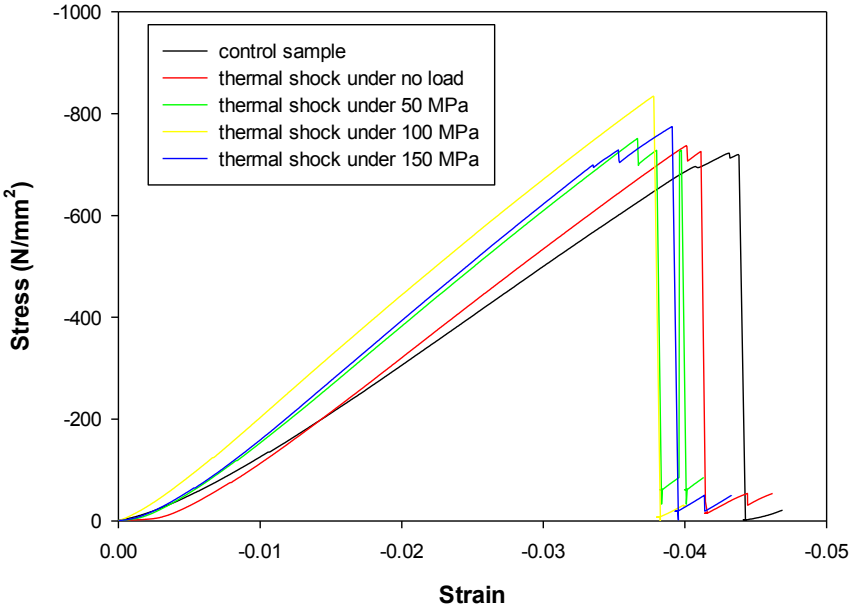

Figure 13: Compression stress – strain graph of all samples

Table 1: Maximum stress of all samples prior to failure.

	Control sample	Thermal shock (no stress applied)	Thermal shock (50MPa applied)	Thermal shock (100MPa applied)	Thermal shock (150MPa applied)
Max. strength (MPa)	722.3	735.4	750.7	833.4	774.7

Conclusions

This paper provides the first data on the mechanical properties of polycrystalline Ti_2AlC after a thermal shock. At room temperature Ti_2AlC the failure mechanism of the material indicated a degree of plastic deformation due to the laminated grains that are composed of a number of thin hexagonal slices that allow shear-slip. The high electrical conductivity of the ceramic enables novel testing of the material at elevated temperature using closed-loop resistive heating; an approach normally limited to metallic materials. The Ti_2AlC was subjected to combined thermal shock and mechanical loading and the current work indicates that Ti_2AlC retains its mechanical properties after thermal shock from 1200^{o}C with a cooling rate higher than 90^{o}C/sec; even when subjected to mechanical loads up to 150Ma. The microstructure and the phases of the samples after the thermal shock were studied

and no significant change or defects was observed supporting the preservation of the mechanical properties. Such ceramics materials therefore show potential for high temperature and high load applications.

References

[1]: M. W. Barsoum et al., Metallurgical and Materials Transactions A, 33A (2002) 2775

[2]: M. W. Barsoum et al., Metallurgical and Materials Transactions A, 31 (2000) 1857

[3]: T.Thomas and C. R. Bowen, J. of Alloys and Compounds, 602 (2014) 72

[4]: L. Liang et al., J. of Wuhan University of Technology-Mater. Sci. Ed., 28 (2013) 882

[5]: W. Garkas et al., Advanced Materials Research, 89-91 (2010) 208

[6]: G. Liu et al., Materials Letters, 61 (2007) 779

[7]: P. Wang, Transactions of nonferrous Metals Society of China, 17 (2007) 1001

[8]: Y. Bai et al, J. of American Ceramic Society, 95 (2012) 358

[9]: X. H. Wang and Y. C. Zhou, Oxid. Met., 59 (2003) 303

[10]: X. H. Wang and Y. C. Zhou, J. of Mat. Science & Technology, 26 (2010) 385

[11]: C. J. Gilbert et al., Scripta Materialia, 42 (2000) 1

[12]: Y. C. Zhou and X. H. Wang, Mat. Res. Innovat., 5 (2001) 87

[13]: http://kanthal.com/en/products/furnace-products-and-heating-systems/refractory-material/

[14]: http://gleeble.com/products/gleeble-3500.html

[15]: BSI 10-1999 (1993)

[16]: M. M. Mahmoud et al., The American Ceramic Society, 252 (2015)

[17]: L. Huet et al., Acta Materialia, 60 (2012) 6266

[18]: H. Zhuet at al., Int. J. Appl. Ceram. Technology, 12 (2015) 403

[19]: M. Naguib at el., J. American Ceramic Society, 94 (2011) 4556

[20]: Evaluation of LS-DYNA Concreate Material Model 159 (2007) US Dep. Of Transportation

[21]: www.instron.com/compression test

[22]: R. Benitez et al., Acta Materialia, 105 (2016) 294